Design of A Bio-Inspired Pneumatic Artificial Muscle with Self-Contained Sensing *

Onder Erin, Nishant Pol, Luis Valle, and Yong-Lae Park, *Member, IEEE*

***Abstract*— Pneumatic artificial muscles (PAMs) are one of the most famous linear actuators in bio-inspired robotics. They can generate relatively high linear force considering their form factors and weights. Furthermore, PAMs are inexpensive compared with traditional electromagnetic actuators (e.g. DC motors) and also inherently light and compliant. In robotics applications, however, they typically require external sensing mechanisms due to their nonlinear behaviors, which may make the entire mechanical system bulky and complicated, limiting their use in simple systems. This study presents the design and fabrication of a low-cost McKibben-type PAM with a self-contained displacement and force sensing capability that does not require any external sensing elements. The proposed PAM can detect axial contraction force and displacement at the same time. In this study, the design of a traditional McKibben muscle was modified to include an inductive coil surrounding the muscle fibers. Then, a thin, soft silicone layer was coated outside of the muscle to protect and hold the sensing coil on the actuator. This novel design measures coil inductance change to determine the contraction force and the displacement. The process can be applied to a variety of existing McKibben actuator designs without significantly changing the rigidity of the actuator while minimizing the device's footprint.**

I. Introduction

McKibben-type pneumatic artificial muscles (PAMs) are a popular actuator in soft robotics [1,2,3]. They are typically constructed with flexible fiber mesh surrounding a stretchable rubber bladder [4,5,6]. The bladder is usually sealed at one end, and an air supply line is connected to the other end, creating a sealed air chamber. Air pressure inside the chamber exerts a radial force on the muscle, resulting in axial contraction based on the limited motion of the surrounding mesh. The flexibility of both the fibers and the bladder allows the muscle to have compliance.

In Traditional pneumatic muscles, sensing displacement and force for axial contraction requires sensors, such as linear encoders and load cells, respectively. These sensors are usually rigid and external to the actuator, significantly increasing the devices' form factor and reducing compliance.

*Research supported by Okawa Foundation Research Grant Award.

O. Erin is with the Department of Mechanical Engineering, Carnegie Mellon University, Pittsburgh, PA 15213, USA (e-mail: author@ ondere@andrew.cmu.edu).

N. Pol is with the Department of Electrical and Computer Engineering and the Robotics Institute, Carnegie Mellon University, Pittsburgh, PA 15213, USA (e-mail: npol@andrew.cmu.edu).

L. Valle is with the Robotics Institute, Carnegie Mellon University, Pittsburgh, PA 15213, USA (e-mail: vallelu@andrew.cmu.edu).

Y.-L. Park is with the Robotics Institute and the Department of Mechanical Engineering, Carnegie Mellon University, Pittsburgh, PA 15213, USA, and also with the Department of Mechanical and Aerospace Engineering, Seoul National University, Seoul, 08826, Korea (e-mail: ylpark@cs.cmu.edu).

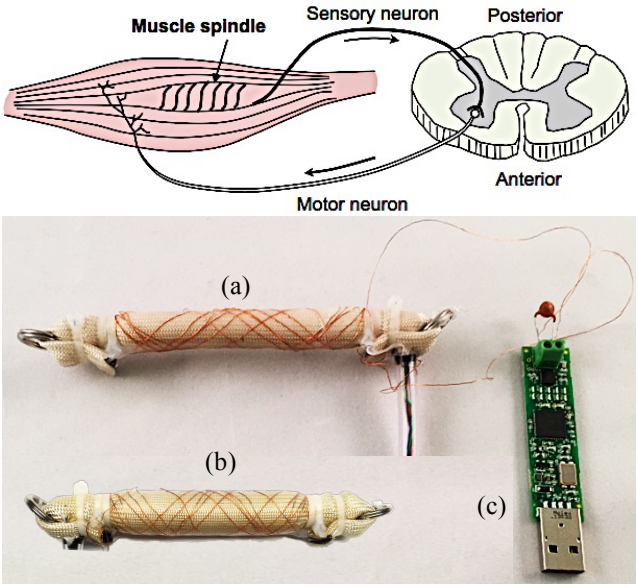

Figure 1. Simplified illustration of the anatomy of a biolocial muscle and a spinal cord showing a muscle spindle (top) and a pneumatic artificial muscle prototype with an inductive sensing coil (bottom). (a) Relaxed muscle. (b) Contracted muscle. (c) Sensor reading module.

This problem has spawned research into sensors that can be integrated into the actuators, forming self-sensing pneumatic muscles [7,8]. In self-sensing actuators, the sensing device shares elements with the actuation device. In actuators with self-contained sensors however, an actuator manufactured without the sensor components still functions for actuation.

The goal of this study is to develop a low-cost integrated sensor that can be applied to an existing PAM design, so the actuator materials are not limited by the sensing mechanism but can be selected for desired actuator performance. The approach presented in this study used a coil of a thin wire wrapped around the muscle. The design was inspired by a biological proprioceptive sensory receptor called a *muscle spindle* (Fig. 1) that detects changes in the length of a muscle, located at the belly of the muscle [9,10]. When the muscle contracts, the muscle spindle detects the displacement of the muscle and send the proprioceptive information to the spinal cord. The advantage this design is low-cost, and the mechanism can be implemented to almost any type of McKibben actuators without being limited by their existing form factors or shapes.

A few examples of sensing mechanisms of self-sensing PAMs include dielectric elastomer, embedded microfluidic elastomer, and conductive fiber mesh.

One approach to building a self-sensing McKibben actuator is to create a capacitor element using dielectric

elastomers [11]. Conductive grease or paint has been used to make electrodes on both sides of the elastomer. As the elastomer is stretched due to pressure or extension, its thickness decreases and area increases, so the capacitance across the elastomer increases. The dielectric elastomer approach, however, limits the selection of the elastomer to thin materials with a high dielectric constant to achieve measurable capacitance.

A PAM with microfluidic sensing has been built using an embedded helical microchannel, filled with a liquid conductor [12,13] – eutectic Gallium-Indium (EGaIn), in the elastomer layer of the bladder. Air pressure inside the bladder stretches the elastomer layer, reducing the cross-sectional area of the embedded microchannel while simultaneously increasing its length [14]. Then, the length of the muscle can be calculated from the resistance change of the microchannel. In this case, the microchannel requires a special manufacturing process that limits the selection of elastomers and fibers for the actuator.

Another approach was to use insulated electrical wires as a replacement of the mesh fibers. The axial contraction force and displacement can be calculated from the changes of the resistance and the inductance of the conductive mesh. Although the fabrication process is relatively simple, the muscle fibers must be chosen to be a type of insulated electrical wires [15].

The theoretical background of the muscle and inductive sensing is introduced next, followed by the manufacturing process, characterization results, and analysis.

II. Theoretical Background

A McKibben artificial pneumatic muscle can be modeled as follows [3, 4]:

$$F = \frac{pb^2}{4\pi n^2}\left(\frac{3}{b^2}\left(\frac{b}{\sqrt{3}}+x\right)^2 - 1\right) \quad (1)$$

where p is the relative pressure of the air chamber with respect to external pressure, b is the muscle fiber weave length, n is the number of turns in the muscle fiber, and x is the displacement.

If l_0 is defined as the length of the muscle for a given air pressure with the absence of exerted axial force, the displacement is defined as:

$$x = l - l_0 \text{ where } l > l_0 \quad (2)$$

In the equation (1), $p, b, and\ n$ are characteristic of the muscle design and setup, assuming steady state operation.

Displacement x can be calculated from the inductance of the wire coil. A long cylindrical inductor can be modeled as

$$L = \frac{\mu_0 N^2 A}{l} \quad (3)$$

where L is the inductance, μ_0 is the permittivity of free space, which is a close approximation to the permittivity of air, A is the cross sectional area, and l is the length. Although typically for inductors the coils are packed sequentially, they can be interweaved as used for the proposed sensor. Interweaved coils are designed in such a way that the inductor current direction is maintained.

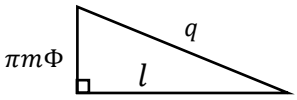

Figure 2. Right triangle formed by a wire weave.

For k number of interleaved coils, each with a length l, or same as the active length of the muscle, and m turns per weave, the effective number of turns is

$$N = mk \quad (4)$$

The cross-sectional area changes with displacement. Let Φ be the diameter of the circular cross section. Since the wire length per weave q must be constant, a right triangle (Fig. 2) is formed for each weave is

$$\Phi = \frac{\sqrt{q^2 - l^2}}{m\pi} \quad (5)$$

Substituting into equation (3):

$$L = \frac{\mu_0 (mk)^2 \pi \left(\Phi/2\right)^2}{l} = \frac{\mu_0 k^2 (q^2 - l^2)}{2\pi l} \quad (6)$$

Solving for $l(L)$:

$$l = \frac{-2\pi L + \sqrt{(2\pi L)^2 + \mu_0^2 k^4 q^2}}{\mu_0 k^2} \quad (7)$$

If the muscle is characterized before use, l_0 is known for the desired pressure, and l can be found from the former equation with the inductor sensor measurement L, so displacement x is known. Using the pressure sensor reading p, the exerted axial force F can be calculated from (1).

For $k^4 \gg \frac{(2\pi L)^2}{\mu_0^2 q^2}$, equation (7) can be approximated as

$$l = -\frac{2\pi L}{\mu_0 k^2} + q \quad (8)$$

which represents a linear relationship between sensor inductance and muscle length. Also, equation (1) can be approximated as a linear spring model

$$F = \kappa(l - l_0) \quad (9)$$

where κ is a linear spring constant. From (1), note κ is dependent on internal air pressure. Combining equations (8) and 9 result in a linear relationship between axial contraction force and sensor inductance

$$F = \alpha L + \beta \quad (10)$$

where

$$\alpha = -\frac{2\kappa\pi}{\mu_0 k^2} \text{ and } \beta = \kappa(q - l_0).$$

III. Design and Manufacturing

For purposes of a complete study, the inductive and pressure sensing elements were built during the muscle manufacturing process. The technique, however, can also be used on an existing muscle.

The inductive sensing element is a wire coil wrapped around the fibers of the PAM. It is important that the wire weave angle matches that of the fibers so the coil expands and contracts with the muscle. This inductive coil is used to

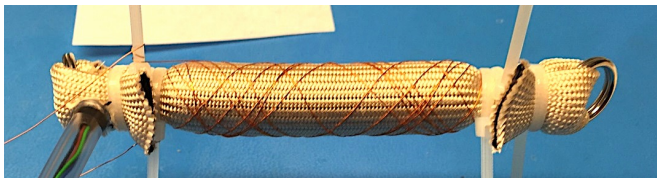

Figure 3. PAM prototype after wrapping wire to build a muscle with a coil wrapped around mesh fibers.

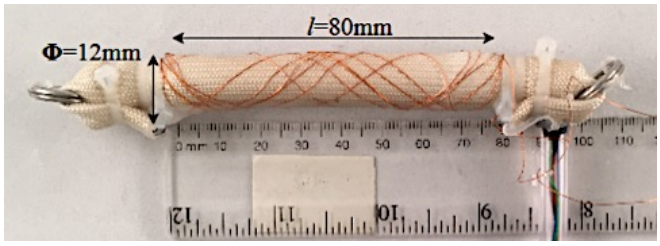

Figure 4. Complete Prototype with dimensions.

determine the muscle length change (i.e. displacement). Optionally, a pressure sensor can be included near the air inlet, to detect the internal air pressure, which can be directly related to the contraction force.

A muscle prototype was constructed from an electrical insulation sleeve (Silicone Flex Glass, Techflex) that has a rubber layer outside a fiberglass mesh. This sleeve was first inverted so the fiberglass mesh was on the outside. A plastic tubing plug was inserted in one end of the sleeve, and an elbow (L-type) tube fitting on the other. Cable ties were used to secure the plug and the fitting, and the excess sleeve was bent to further seal the internal air chamber.

The Installation procedure for the coil is as follows:

First, the muscle was pressurized to the maximum designed pressure, 410 kPa relative to the ambient room pressure. This internal air pressure should be maintained during the manufacturing process, either by using a valve, or keeping the muscle attached to a pressurized air supply.

Second, an insulated wire was wrapped around the muscle to match the weave angle of the muscle fiber (Fig. 3). The wire should be thin, for example, our prototype used a 34-AWG magnet wire since thinner wires have less impact on the flexibility and the behavior of the muscle. For the PAM prototype in this study, a weave angle of approximately 32° was used, resulting in 1.6 turns per length (Fig. 4). Multiple weaves were used to increase the number of turns, and consequently the inductance. The prototype had 12 weaves, resulting in 19.2 turns.

Finally, silicone elastomer (Ecoflex-0010, Smooth-On) in a liquid state was poured over the wire and the muscle fibers. This method was chosen instead of dipping so the wire position would not shift. The muscle was hung vertically and flipped every 15 minutes for an hour for the silicone to cure uniformly. Once the silicone has cured after 24 hours, the muscle was depressurized and ready for use. A calibrated absolute pressure sensor was installed on the air supply line to provide an estimate of internal air pressure.

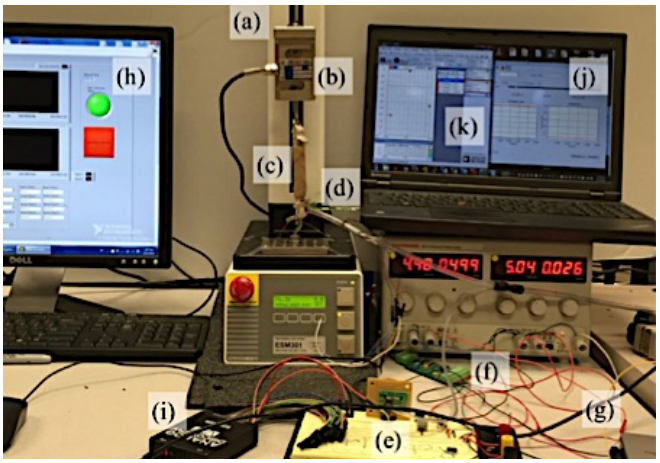

Figure 5. Muscle Test Setup: (a) Test Stand, (b) Load Cell, (c) PAM, (d) Inductance to Digital Converter, (e) External Pressure Sensor, (f) Load Cell Amplifier, (g) NI DAQ for Load Cell, (h) Load Cell GUI, (i) Oscilloscope for Pressure Sensor, (j) Oscilloscope GUI, (k) LDC1000 GUI.

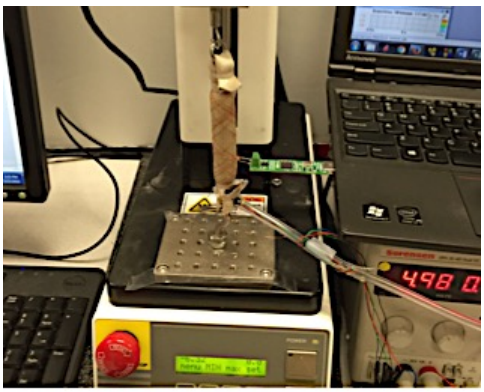

Figure 6. Close-up showing PAM in test stand and Inductance to Digital Converter evaluation module.

IV. Characterization Procedure

The inductive sensor was characterized by measuring the sensor inductance and the exerted axial contraction force, while varying the muscle length, for three different pressures. As shown in Figs. 5 and 6, the muscle was mounted in a motorized materials test stand (ESM303, Mark-10) and a load cell (STL-50, AmCells) for setting the length of the muscle and for measuring the applied force, respectively. Inductance was measured using an inductance to digital converter (LDC1000, Texas Instruments) and its graphical user interface (GUI) software. The air pressure was measured with an external absolute pressure sensor (MPXH6400A, NXP/Freescale Semiconductor).

Fig. 7 shows the overall schematic for data acquisition. At the beginning of each test, the pressurized muscle was slightly pre-strained so the reference load cell reading was above 0 N. Then, the muscle displacement was increased as axial contraction force, air pressure, and inductance were measured. After reaching the unpressurized muscle length, the muscle displacement was reduced and data recorded until an absence of axial contraction force. This test was performed at three different air pressures: 260 kPa, 300 kPa, and 370 kPa. Ambient room pressure was 96 kPa.

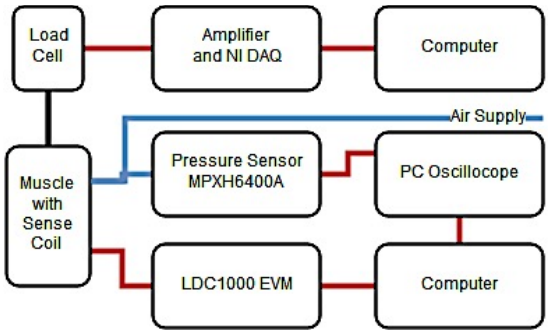

Figure 7. The schematic of data acquisition network used in the experiments.

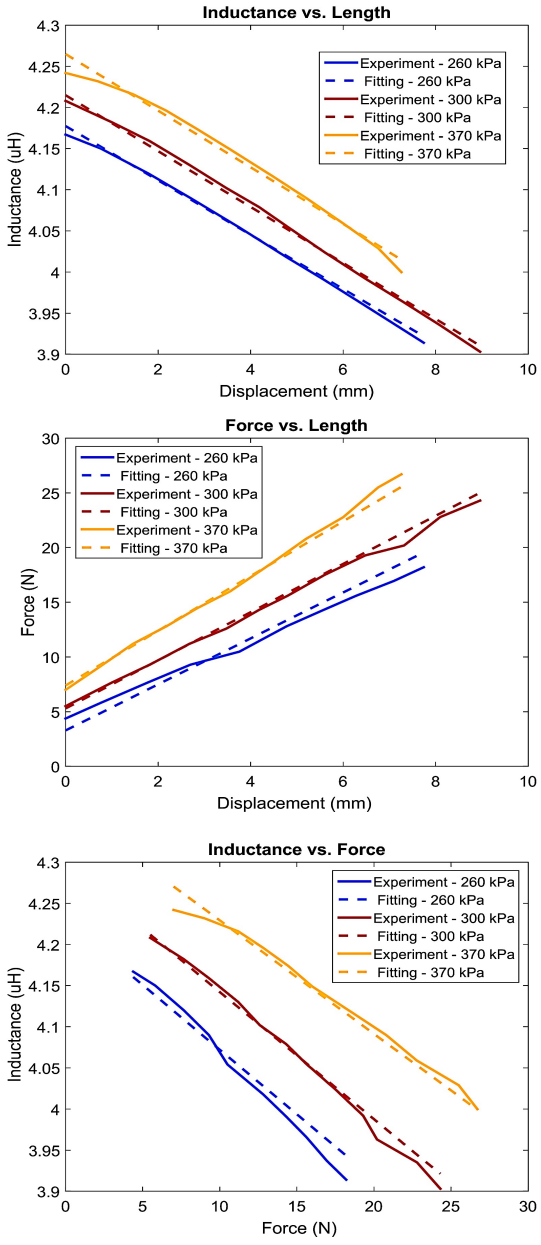

Figure 8. The experimental results for the PAM tested at three air supply pressures, as displacement was increased. The experimental results show a linear relationship between axial contraction force and inductance. R^2 >0.99 for all linear regression models.

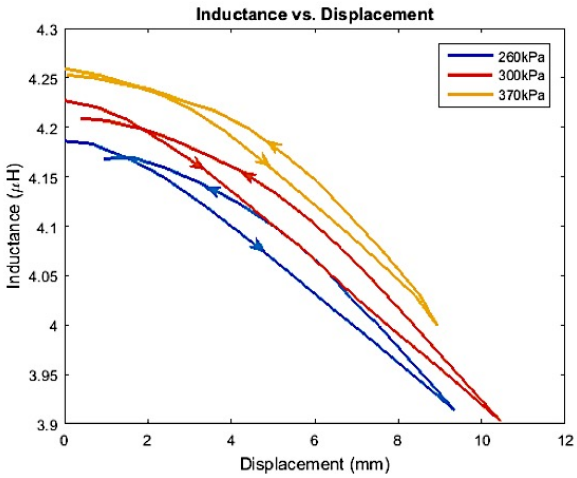

Figure 9. The experimental results for the PAM tested at three air supply pressures, as displacement was increased. The experimental results show a linear relationship between axial contraction force and inductance. R^2 >0.99 for all linear regression models.

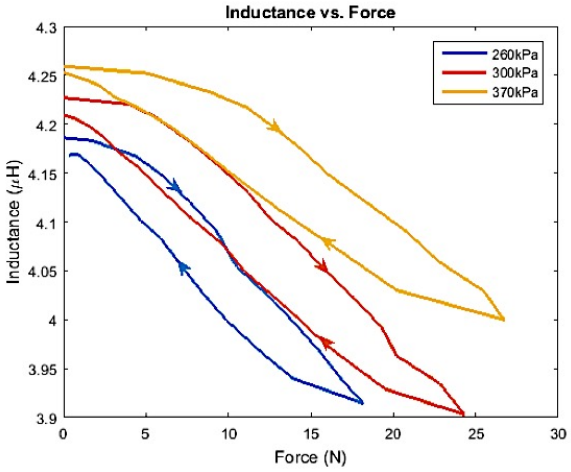

Figure 10. The experimental results for the PAM tested at three air supply pressures, as displacement was increased. The experimental results show a linear relationship between axial contraction force and inductance. R^2 >0.99 for all linear regression models.

V. Characterization Results

As derived in Section II, the theoretical model indicated a linear relationship between the axial contraction force and the coil inductance since the underlying relationships for contraction force versus displacement and inductance versus displacement are linear. The experimental results supported the theoretical predictions (Fig. 8).

The α and β values in equation (10) can be determined from the experimental results (TABLE I). The coefficients indicate that increasing the air pressure results in higher sensitivity in terms of force and inductance for the tested PAMs.

Due to the linear relationship between the contraction force and the coil inductance, PAMs with sensors can be arranged in series or parallel configurations. This enables the user to design a configuration with a force and displacement profile best suited for the application.

We also tested the PAM and sensor for hysteresis by increasing and decreasing the displacement of the muscle and measured the inductance change for the displacement and the force (Figs. 9 and 10). In both cases, the sensor showed hysteresis.

The hysteresis level was higher with the force change than with the displacement. The major source of the hysteresis is the geometry change of the muscle from the expansion of the polymer bladder. Therefore, the hysteresis can be attributed rather to the actuator than to the sensing element and therefore can be addressed by changing the bladder material or the configuration of the muscle fibers.

Although the test was conducted under steady state conditions where samples were taken several seconds apart, it is likely that the wire winding did not uniformly expand and contract with the muscle fiber weave. Based on the pattern shown in Fig. 8, the wire winding expanded more than it contracted, for most of the working range of the muscle.

VI. Conclusion

An inductive sensor for a McKibben type PAM was integrated into an existing muscle design. The sensor used an interwoven coil to increase the number of turns while maintaining the weave angle of the PAM fibers. The contraction displacement and the force of the PAM can be calculated from the measured coil inductance and from the coil inductance and the internal air pressure, respectively.

A linear relationship between the inductance and the displacement was observed with slight hysteresis. Similarly, a linear relationship between the inductance and the contraction force was observed with a slightly greater hysteresis level. Both relationships agreed with the derived theoretical model predictions.

Although we presented the steady state behavior of the muscle in this study, further testing will focus on exploring the cause of hysteresis if the coil pattern stays constant over multiple cycles. Furthermore, the dynamic response of the PAM and inductive sensor combination will be studied to evaluate the use of the proposed system in dynamic applications. If the design proves to show reliable steady state and transient response characteristics, the sensor will be an inexpensive alternative to traditional load cells that have been externally integrated with the muscle with relatively high cost and increased form factors.

TABLE I. α AND β VALUES

	Pressure (kPa)		
	260	***300***	***370***
α	-6.36 x 10^7	-6.47 x 10^7	-7.26 x 10^7
β	269.13	278.04	317.09

References

[1] D. Rus and M. Tolley, "Design, fabrication and control of soft robots," *Nature*, Vol. 521, pp. 467-475, 2015.

[2] C. Majidi, "Soft robotics: a perspective—current trends and prospects for the future," *Soft Rob.*, Vol. 1, No. 1, pp. 5-11, 2013.

[3] M. Wehner, M. T. Tolley, Y. Menguc, Y.-L. Park, A. Mozila, Y. Ding, C. Onal, R. F. Shepherd, D. Rus, G. M. Whitesides, and R. J. Wood, "Pneumatic energy sources for autonomous soft robots and wearable soft robots," *Soft Rob.*, Vol. 1, No. 4, pp. 263-274, 2013.

[4] C. Chou, B. Hannaford, "Measurement and modeling of McKibben pneumatic artificial muscles," *IEEE Trans. Rob. Autom.*, vol. 12, No. 1, pp. 90-102, 1996.

[5] B. Tondu, "Modelling of the McKibben artificial muscle: A review," *J. Intell. Mate. Syst. Struct.*, Vol. 23, pp. 225-253, 2012.

[6] Y.-L. Park, B. Chen, C. Majidi, R.-J. Wood, R. Nagpal, and E. Goldfield, "Active modular elastomer sleeve for soft wearable assistance robots," *Proc. IEEE/RSJ Int. Conf. Intell. Rob. Syst.*, pp. 1595-1602, Vilamoura, Portugal, 2012.

[7] S. Kuriyama, M. Ding, Y. Kurita, J. Ueda, and T. Ogasawara, "Flexible sensor for McKibben pneumatic artificial muscle actuator," *Int. J. Autom. Technol.,* Vol. 3, No. 6, pp. 731-740, 2009.

[8] T. Akagi, S. Dohta, Y. Kenmotsu, Y. Kenmotsu, and M. Yoneda, "Development of smart inner diameter sensor for position control of McKibben artificial muscle," *Procedia Eng.*, Vol. 41, pp. 105-112, 2012.

[9] P. B. C. Matthews, "Muscle spindles and their motor control," *Physiol. Rev.*, Vol, 44, No. 2, pp. 219-288, 1964.

[10] N. A. Sachs, G. E. Loeb, "Development fo a BIONic muscle spindle for prosthetic proprioception," IEEE Trans. Biomed. Eng., Vol. 54, No. 6, pp. 1031-1041, 2007.

[11] N. C. Goulborne et al, "Self-sensing McKibben actuators using dielectric elastomer sensors," in *Proc. SPIE 6524 Electroactive Polymer Actuators and Devices.*, San Diego., CA, April 2007.

[12] Y.-L. Park, B. Chen, and R. J. Wood, "Design and fabrication of soft artificial skin using embedded microchannels and liquid conductors," *IEEE Sens. J.*, Vol. 12, No. 8, pp. 2711-2718, 2012.

[13] J.-B. Chossat, H.-S. Shin, Y.-L. Park, and V. Duchaine, "Soft tactile skin using an embedded ionic liquid and tomographic imaging," *ASME J. Mech. Rob.*, Vol. 7, No. 2, 021008 (9 pp.), 2015

[14] Y.-L. Park, R. J. Wood, "Smart pneumatic artificial muscle actuator with embedded microfluidic sensing," *Proc. IEEE Sens. Conf.*, pp. 689-692, Baltimore, MD, 2013.

[15] W. Felt, C. D. Remy, "Smart braid: air muscles that measure force and displacement," *Proc. IEEE/RSJ Int. Conf. Intell. Rob. Syst.*, Chicago, IL, 2014, pp. 2821-2826.